A RELIABLE METHOD TO COUNT TRACKS FROM SOLID STATE NUCLEAR TRACK DETECTORS IN THE MEASUREMENT OF RADON CONCENTRATION

Marcos Aurélio de Andrade Pinheiro[1] and Kátia Cardozo[2]

Instituto de Engenharia Nuclear, IEN - CNEN
Rua Hélio de Almeida, 75
21941-906 Rio de Janeiro, RJ
[1]pinheiro@ien.gov.br, [2]cardozo@ien.gov.br

ABSTRACT

Radon is an alpha emitter that accounts for about 50% of internal dose for man and is an important cause of death by lung cancer. For this reason, reliable methods to measure the radon concentration in the air are of great concern to the area of radiological protection. From the radiological point of view, the ^{222}Rn is more relevant than the ^{220}Rn because the latter has a shorter half-life and thus is less likely to reach the human body. This paper describes the method used at the Instituto de Engenharia Nuclear (IEN) to measure the ^{222}Rn concentration (Bq.m^{-3}) in occupational and domestic environments. This method is based on the well-known track etch technique and the detector employed is the LEXAN plastic. It is described the electrochemical process used to reveal the tracks generated at the detector surface by the incidence of the alpha particles from radon and its progeny decay. In order to count the tracks, a program based on image processing techniques was developed at the IEN. This program processes the grey-scale images that are obtained by scanning the revealed detectors. The counting uncertainty of this program was estimated by comparing its results with those found by manual counting. As will be seen, this program gives reliable results even if the tracks overlap and the electrochemical revelation process provides tracks with high shape distortion. Other issues relating to the performance of this program are also discussed.
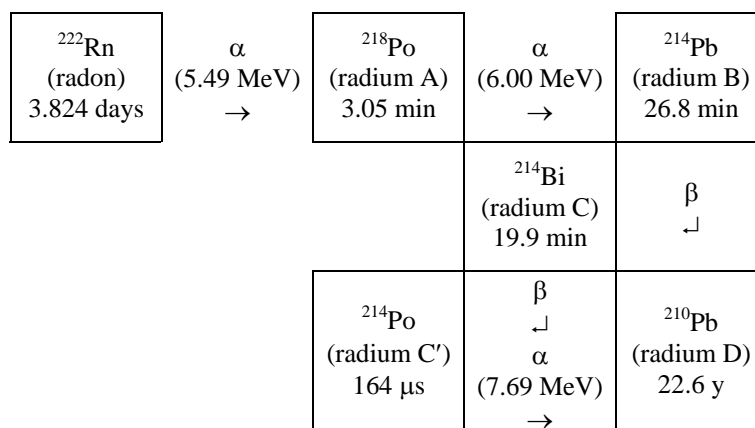
1. INTRODUCTION

The radioactive noble gas radon, ^{222}Rn, is an isotope from the uranium chain (Fig. 1) and is present in all indoor and outdoor environments. Consequently, the human being is put, along all his life, under continuous exposure to this radioactive gas. Owing to the risks of lung cancer, a world-wide concern arose aiming to minimize the human exposure to radon by following the ALARA principle, specially regarding public exposure [1]. Remedial actions taken by a regulatory authority or by an intervening organization may be required to reduce or to avoid additional doses for the public as well for workers exposed occupationally [2].

Radon whose emitted alpha particles produce nuclear tracks in a solid surface can be detected by a solid state nuclear track detector (SSNTD). Nuclear tracks were first observed by Young [3]. In 1965 General Electric researchers found that nuclear tracks generated by alpha particles [4] could be chemically revealed [5].

Doses due to radon are directly related to the concentration of this gas in the air. To measure this concentration, solid state track detectors are a cheap and common choice, since these detectors do not require power supplies, nor special cares to handle or to use. In this work, a polycarbonate trade-named LEXAN was used as passive plastic detector, because of its

availability and its property of registering tracks generated by the alpha decay of radon and its progeny.

Section 2 describes the electrochemical process employed to reveal the tracks generated at the detector surface by the alpha particles from radon and its progeny [6]. The problem of counting the tracks in an image is briefly commented in Section 2.2. The performance of the program developed at the IEN is discussed in Section 3. The conclusions of this work are in Section 4.

^{222}Rn (radon) 3.824 days	α (5.49 MeV) →	^{218}Po (radium A) 3.05 min	α (6.00 MeV) →	^{214}Pb (radium B) 26.8 min
			^{214}Bi (radium C) 19.9 min	β ↵
		^{214}Po (radium C′) 164 μs	β ↵ α (7.69 MeV) →	^{210}Pb (radium D) 22.6 y

Figure 1. Part of the uranium chain showing radon and its progeny.

## 2. FUNDAMENTALS AND METHODOLOGY

2.1. Radon Measurements

The LEXAN detectors used in this work have a round shape with 2.54 cm of diameter. They are placed into diffusion chambers closed by a hydrophobic fiberglass filter. The design of these chambers is such that only radon diffuses through the filter and reach the detector. Aerosols and attached radon decay products are deposited on the filter and do not enter the chamber.

When the alpha particles emitted from radon and its short-lived progeny pass through the detector, they transfer their energy to the material causing the break of the chemical bonds of the polymer. The tracks so formed, however, are not visible. After submitting the detector to an adequate chemical attack, the tracks become visible, since the chemical reaction is faster in the region where the chemical bonds were broken. At the IEN, the LEXAN detectors are arranged in an electrochemical cell where they are put in contact with a KOH 8M/ethanol (4:1) solution. Initially, the detectors stay there for one hour with no voltage applied (pre-etching). Subsequently, an alternate electric field of 800 V and 3 kHz is applied to the cell for 3 hours.

2.2. Image Counting

Once the detectors are revealed, the tracks become visible and thus can be counted in order to derive the radon concentration. To perform the automatic counting of the tracks, a digital image is generated by scanning the detector against a black background to highlight the tracks. As an example, it is depicted in Fig. 2 the negative of an image so obtained with a resolution of 1200 pixels per inch (ppi). By using the LEXAN detector and under the etching conditions found at the IEN, there is a saturation of tracks at 2000 tracks.cm^{-2}. Above this value, the detection efficiency decreases, because the number of overlapped tracks increases. The counting is converted to radon concentration by using the factor 13.8 tracks.cm^{-2}.kBq^{-1}.m^{3}.day, obtained from the calibration of the detector with a radon standard.
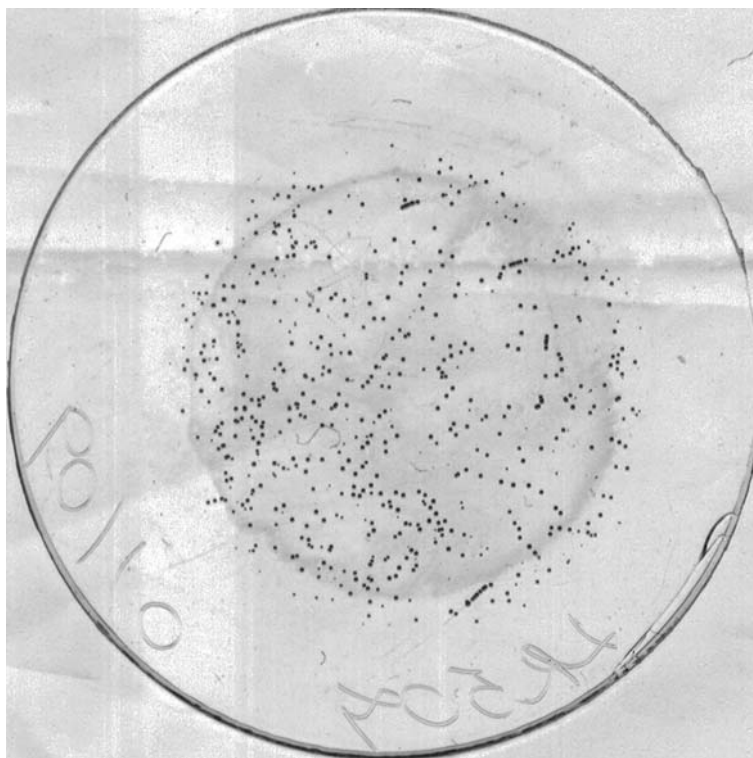
Figure 2. Negative of an image obtained by scanning a revealed LEXAN detector (the black spots are radon tracks).

The problem of automatically count the tracks of the images obtained as described above is not trivial. The difficulties involved in this task are exposed with the aid of Fig. 3. In this example, the two overlapped tracks encircled in Fig. 3a appear magnified in the gray-scale image of Fig. 3b, where each square represents a pixel with intensity ranging from black (lowest) to white (highest) [7]. A normalized three-dimensional view of Fig. 3b is depicted in Fig. 3c. Besides being randomly positioned and having irregular shapes, the tracks are not generally flat, so that they may exhibit more then one peak. This occurs in Fig. 3b and 3c, where the local maxima of interest of the selected overlapped tracks are denoted as A, B, C,

and D. Consequently, a counting strategy based exclusively on the search of the total number of peaks of an image does not provide a reliable counting result.


(a)

(b)

(c)
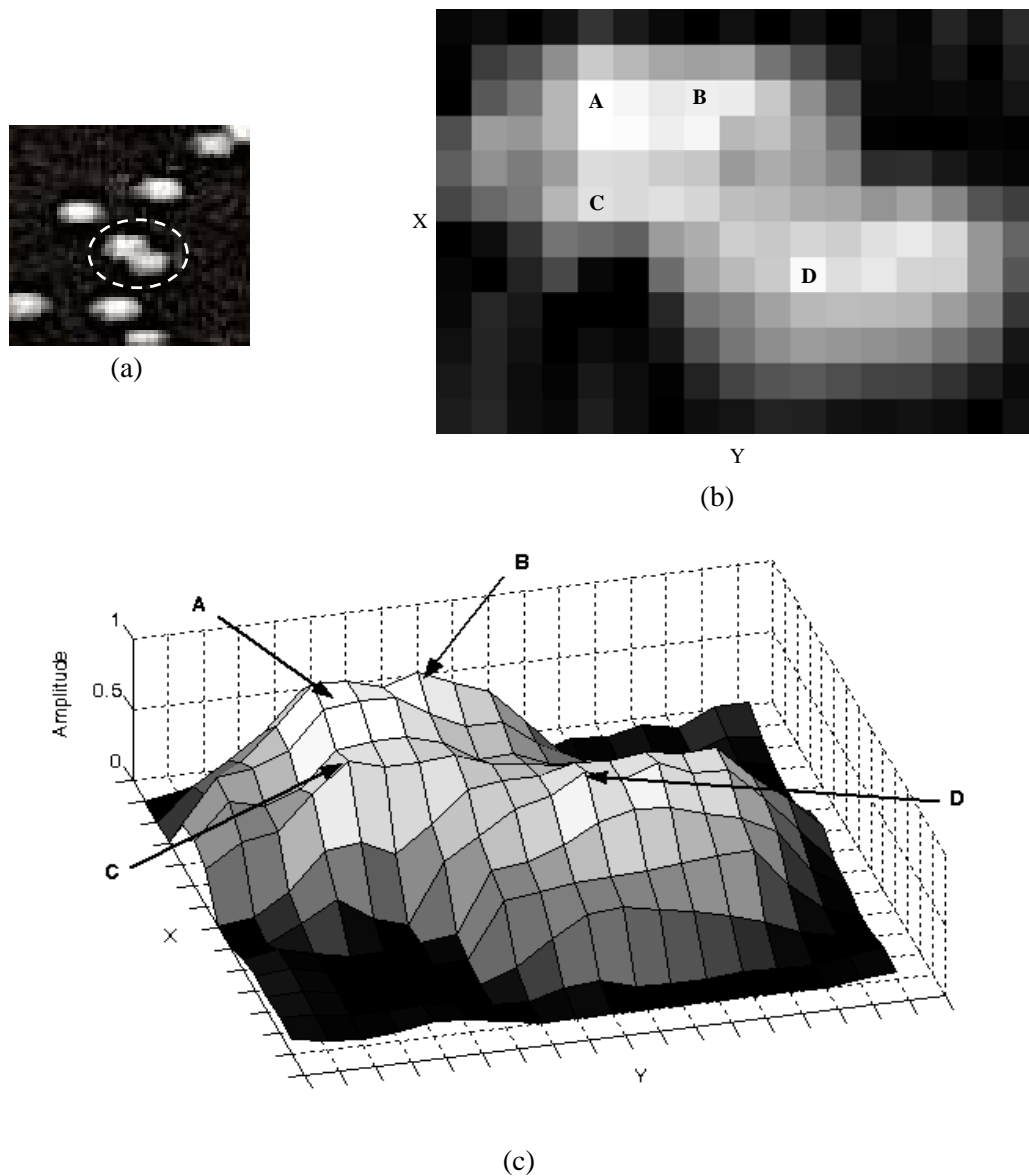
Figure 3. Track overlapping (a) detail; (b) magnification of (a); (c) three-dimensional view of (b).

Additional difficulty to the problem in question is imposed by the occurrence of overlapping tracks. For an experienced observer, the object selected in Fig. 3a would probably be regarded, according to some adequate criterion, as two tracks overlapped, i.e., one track formed by the peaks A, B, and, C, and the other track by the peak D. For a computer algorithm, however, the existence of multiple local maxima in the overlapped tracks may lead to a false conclusion. This is because the valleys between the peaks of the tracks generally have random depth and breadth, so that it is sometimes hard to assure if a certain valley

separates two overlapped tracks or the peaks of a same track. Thus, the object selected in Fig. 3a could be wrongly counted by a computer program as just one track, as suggests the large mass in Fig. 3c, or even as four overlapped tracks centered on A, B, C, and D (see Fig. 3b). Overlapping is specially relevant in images with a high density of tracks. In low density images, counting errors due to overlapping may not be significant to the calculation of the radon concentration. Since the correct identification of overlapped tracks generally introduces a significant computational overload, a compromise solution may be adopted, at the expense of the accuracy, to do not increase prohibitively the overall execution time of the program. Additionally to overlapping, spurious tracks due to scratches and other higher energy particles are also sources of errors. In general, the random nature of the many factors involved prevents the algorithm from reaching the true value of the total number of tracks, so that an automate counting will generally give just an estimate of this true value.

3. RESULTS

A computer program was developed at the IEN to count the images generated as described in Section 2. This program has been extensively used by the Radon Laboratory of the IEN and has given satisfactory results within a certain error margin. The performance of the program is discussed with the aid of Fig. 4 and 5 below, where each counted track is properly marked.
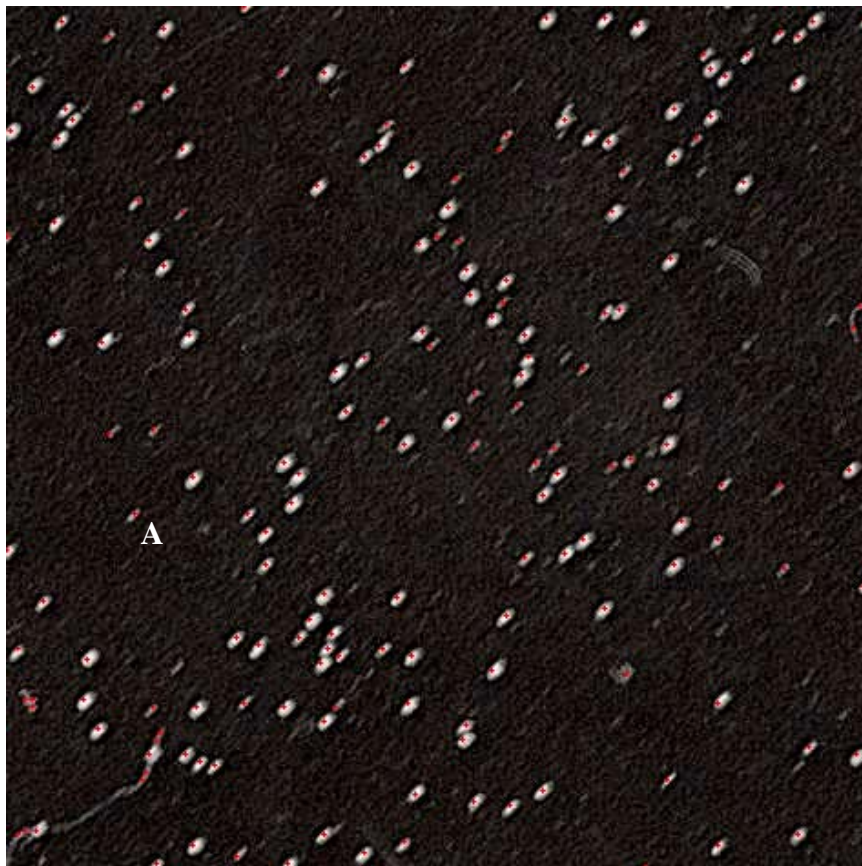
**Figure 4. Image processed by the program developed at the IEN
(the red marks indicate the counted tracks).**

(a)

(b)
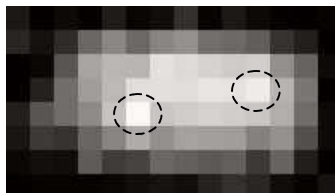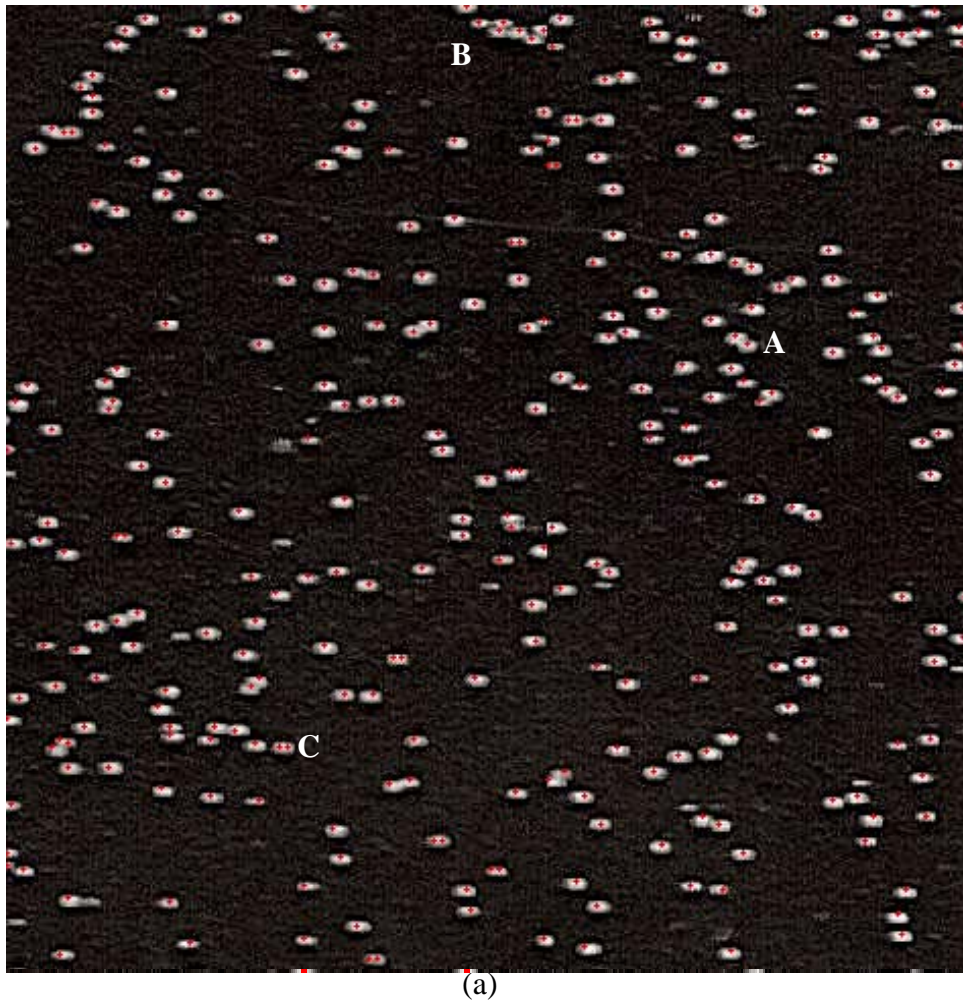
Figure 5. (a) Example of an image counted by the program developed at the IEN. (b) Detail of the track denoted by letter C in (a).

Figure 4 is a region of interest of an image obtained by scanning a LEXAN detector rotated by 45°. Clearly, the program was able to detect most tracks, despite they are distorted and have an unfocused appearance. This image and other results not presented here indicate that, under certain limits, the program has low sensitivity to the shape of the tracks. As a prove of consistency of the program, no marks were assigned to the noisy black background. Some scratches, however, were marked because their intensities are comparable to those of minor

tracks, like "A" in Fig. 4. These minor tracks are caused by particles with higher energies or with low incidence angles (see Fig. 1) [8]. It is out of the scope of this paper to give a more detailed explanation about the appearance of these minor tracks.

Among other features, Fig. 5 exemplifies the performance of the mentioned program in relation to overlapped tracks. The object identified by the letter A in Fig. 5a is the same encircled in Fig.3a. As shows Fig. 5a, many overlapped tracks, like A and those in the group denoted by B, were correctly identified by the program. The object denoted by the letter C is a single track. It was wrongly recognized by the program as two overlapped tracks because, as indicate the two encircled objects in Fig. 5b, this track has two peaks separated by a valley with breadth and depth relatively high.

To evaluate the accuracy given by the mentioned program, some images were also manually counted by an experienced technician. Notice that this kind of comparison is acceptable since one of the aims of this paper is to asses only the performance of the program. Future works will be done to verify the accuracy of radon concentration measurement. The results concerning 32 images are listed in Table 1. In the column denoted by N are the counting results obtained with the aid of the program. The differences between these values and the found in the manual counting are listed in column E. The relative error, η, was calculated as

$$\eta = \left| \frac{E}{N} \right| 100\%. \tag{1}$$

Table 1. Counting results from the program developed at the IEN

IMAGE	N	E	η (%)
1	62	-4	6.5
2	67	+1	1.5
3	74	-3	4.1
4	78	+5	6.4
5	82	-2	2.4
6	96	-5	5.2
7	97	-3	3.1
8	99	-3	3.0
9	99	-4	4.0
10	100	+5	5.0
11	101	+1	1.0
12	101	-5	5.0
13	127	-6	4.7
14	127	-2	1.6
15	137	-1	0.7
16	139	-3	2.2
17	144	-8	5.6
18	148	-4	2.7
19	150	+0	0.0
20	173	-9	5.2

Table 1. Counting results from the program developed at the IEN (cont.)

IMAGE	N	E	η (%)
21	177	-6	3.4
22	209	+0	0.0
23	211	-6	2.8
24	231	+2	0.9
25	260	+5	1.9
26	285	+4	1.4
27	313	-8	2.6
28	543	+7	1.3
29	550	-6	1.1
30	711	-10	1.4
31	816	-6	0.7
32	1033	-36	3.5
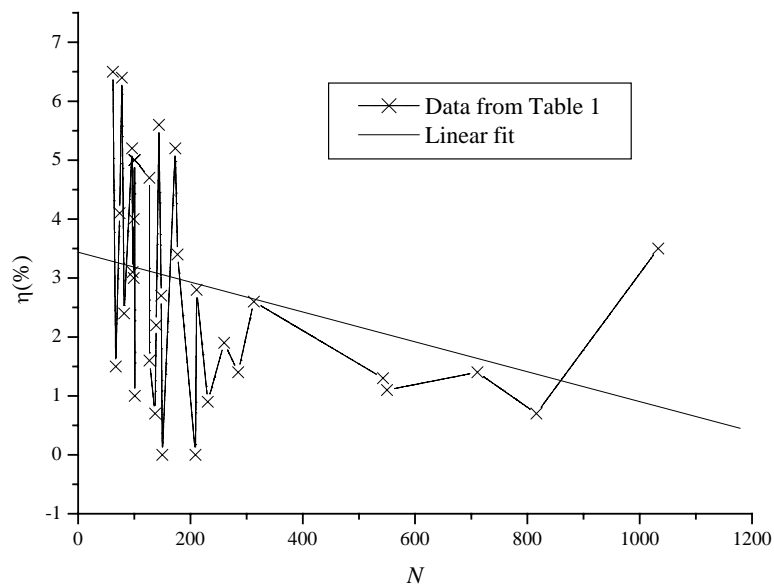
Figure 6. Plot obtained from Table 1: Relative error (η(%)) versus Counting results (N).

The data listed in Table 1 were used to plot, in Fig. 6, the relative error, η, against the counting results, N, given by the program. Most of the images used (from 1 to 27) have N less than 400 so that the points appear concentrated in the left side of Fig. 1. The linear fit reveals an inverse proportionality between N and η. This behavior indicates that, in the range of N considered, the program does not commit, within a certain tolerance, more errors as the image becomes more dense. Actually, it follows from Eq. 1 that η tends to decrease provided that an increase in N does not result in a great number of errors (E). As an example, images 20 and 30 in Table 1 have similar η, but their counting results, N, are significantly different.

Since most η are below 4% and even the greatest η found, 6.5% in image 1, is considered acceptable, it is possible to conclude that the program gives reliable counting results within a certain tolerance.

4. CONCLUSIONS

The relatively low sensitivity of the program to the shape and the size of the tracks allows to alleviate the requirements of the electrochemical etching system. According to the results above shown in this paper the program developed at IEN provides reliable counting results. Notice that this paper focus on the assessment of the performance of the program only. Future experiments will be done to verify the accuracy of the radon concentration measurement.

REFERENCES

[1] INTERNATIONAL COMMISSION ON RADIOLOGICAL PROTECTION, 1990 *Recommendations of the International Commission on Radiological Protection*, Publication 60, Pergamon Press, Oxford and New York (1991).

[2] FOOD AND AGRICULTURE ORGANIZATION OF THE UNITED NATIONS, INTERNATIONAL ATOMIC ENERGY AGENCY, INTERNATIONAL LABOUR ORGANISATION, OECD NUCLEAR ENERGY AGENCY, PAN AMERICAN HEALTH ORGANIZATION, WORLD HEALTH ORGANIZATION, *International Basic Safety Standards for Protection against Ionizing Radiation and for the Safety of Radiation Sources, Safety Series*, No. 115, IAEA, Vienna (1996).

[3] Young, D. A., "Etching of Radiation Damage in Lithium Fluoride," *Nature*, **V. 182**, pp 375-377 (1958).

[4] Fleischer, R. L., Price, P. B. and Walker, R. M., "Ion Explosion Spike Mechanism for Formation of Charged-Particle Tracks in Solids," *J. Appl. Phys.*, **V. 36**, pp. 3645 (1965).

[5] Fleischer, R. L., Price, P. B. and Walker, R. M., "Nuclear Tracks in Solids Principles and Applications," University of California Press (1965).

[6] Dadvand, N. and Sohrabi, M., "Effects of Pre-soaking on Characteristics of Lexan Polycarbonate," *Appl. Radiat. Isot.*, **V. 48**, No. 8, pp 1127-1131 (1997).

[7] Gonzales, R. C., Woods, R. E., *Digital Image Processing*, Prentice-Hall, New Jersey (2000).

[8] Hosseini Pooya, S. M., Afarideh, H., Taheri, M. And Kardan, M. R., "Passive α-particles spectrometry by polycarbonate SSNTD using new etching conditions," *Radiation Physics and Chemistry*, **V. 77**, pp. 949-953 (2008).